Journal of Hazardous Materials 415 (2021) 125629

Contents lists available at ScienceDirect

Journal of Hazardous Materials

journal homepage: www.elsevier.com/locate/jhazmat

Research Paper

Health risk assessment of heavy metal(loid)s in park soils of the largest megacity in China by using Monte Carlo simulation coupled with Positive matrix factorization model

Jingling Huang, Yuying Wu, Jiaxun Sun, Xiao Li, Xiaolei Geng, Menglu Zhao, Ting Sun, Zhengqiu Fan *

Department of Environmental Science and Engineering, Fudan University, Shanghai 200433, China

ARTICLE INFO

Editor: Dr. S Nan

Keywords:
Pollution assessment
Source apportionment
Probabilistic health risk
Urban park

ABSTRACT

Urban Parks are important places for residents to engage in outdoor activities, and whether heavy metal(loid)s (HMs) in park soils are harmful to human health has aroused people's concern. A total of 204 topsoil samples containing nine HMs were collected from 78 urban parks of Shanghai in China, and used to assess the health risks caused by HMs in soils. The results revealed that the Hg, Cd and Pb were the main enriched pollutants and posed higher ecological risks than the other HMs. Four HM sources (including natural sources, agricultural activities, industrial production and traffic emissions) were identified by combining the Positive matrix factorization model and Correlation analysis, with the contribution rate of 48.24%, 7.03%, 13.04% and 31.69%, respectively. The assessment of Probabilistic health risks indicated that the Non-carcinogenic risks for all populations were negligible. However, the Total carcinogenic risk cannot be negligible and children were more susceptible than adults. The assessment results of source-oriented health risks showed that industrial production and traffic emissions were estimated to be the most important anthropogenic sources of health risks for all populations. Our results provide scientific support needed for the prevention and control of HM pollution in urban parks.

1. Introduction

Urban parks are playing an increasingly important role in enriching the daily leisure life of urban residents and balancing the urban ecosystem (Brtnicky et al., 2019). Unlike single-family houses in western countries, most Chinese urban residents live in high-rise buildings (Jin et al., 2019) and enjoy most of their outdoor activities in parks. Particularly during the pandemic period, such as the outbreak of COVID-19, urban parks provide people with a safe haven for outdoor activities and social contact, and become an important place for residents to relax and entertain (Shoari et al., 2020; Xie et al., 2020). However, as an important environmental medium, park soils may represent a pathway for urban residents to be exposed to various potential pollutants, such as heavy metal(loid)s (HMs) (Davis et al., 2009; Liu et al., 2018).

HMs are the most widely distributed components of concern in soils, and they pose a threat to human health through long-term exposure by three pathways including hand-to-mouth ingestion, breathing inhalation and dermal contact (Gu et al., 2017; Wang et al., 2019a). HMs have high persistence and biotoxicity, which may cause a variety of diseases and even cancer (Lin et al., 2018). Previous studies have shown (Houston, 2012; TzuHsuen et al., 2020; Wallace et al., 2020; Yao et al., 2020) that exposure to HMs (such as Hg, As, Pb and Cd) can affect the function of kidney, lungs or other organs, leading to skeletal, cardiovascular and cerebrovascular diseases (WHO, 2020; Yang et al., 2019). Therefore, understanding the pollution levels and health risks of HMs is critical for the safety of human health, especially children who have relatively frequent hand-mouth behaviors and are more likely to accidentally ingest the HMs in soils (Jin et al., 2019).

To effectively control the health risks caused by soil HMs, it is necessary to identify and quantify the potential pollution sources, especially those posed by human activities (Hou and Li, 2017). Existing

List of Abbreviations: HMs, Heavy metal(loid)s; PMF, Positive matrix factorization; HRA, Health risk assessments; I_{geo}, Geo-accumulation index; EF, Enrichment factor; INI, Improved Nemerow index; RI, Potential ecological risk index; NCR, Non-carcinogenic risk; CR, Carcinogenic risk; HI, Hazard index; TCR, Total carcinogenic risk; CV, Coefficient of variation; ABV, Average background value.

* Corresponding author.
E-mail address: zhqfan@fudan.edu.cn (Z. Fan).

https://doi.org/10.1016/j.jhazmat.2021.125629
Received 1 December 2020; Received in revised form 27 February 2021; Accepted 7 March 2021
Available online 11 March 2021

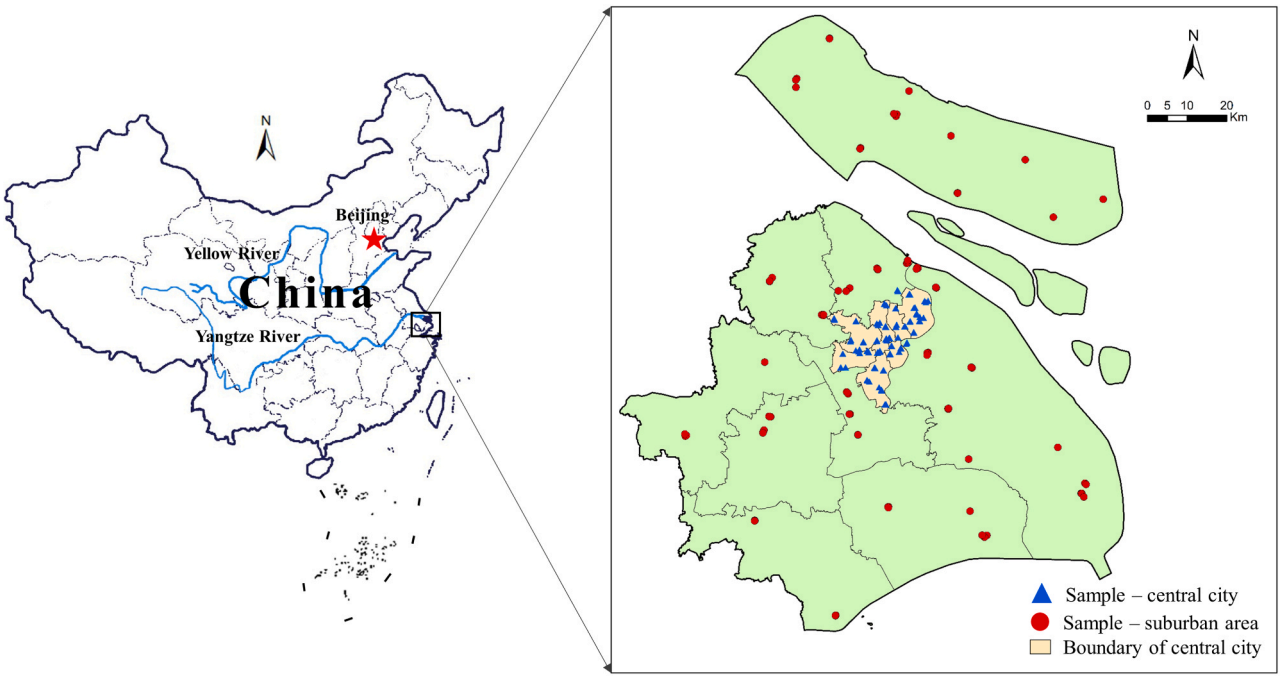

Fig. 1. Sampling locations of 78 urban parks in the study area.

studies indicate that some efforts have been made to identify the source of HMs in soils (Davis et al., 2009; Tian et al., 2018; Yadav et al., 2019). The Positive matrix factorization (PMF) model recommended by USEPA (2014a) can get the non-negative source contribution of each data point and help to apportion the source contribution to each element (Tian et al., 2018). Therefore, in recent years, it has been gradually used for source analysis of HMs (Guan et al., 2018; Huang et al., 2018; Li and Feng, 2012). However, the PMF model mainly relies on researchers' interpretation for the background data of study area, so its applicability and accuracy are limited (Li et al. 2020). Then, on the basis of combining PMF model and Pearson correlation analysis, a comprehensive method was developed to improve the accuracy of source identification in this study.

Meanwhile, most existing health risk assessments (HRA) rely on the traditional models with some certain deterministic parameters (Brtnicky et al., 2019; Gu et al., 2017; Wang et al., 2016). However, due to the uncertainty of concentrations and specific individual variations, it is hard to apply point estimation method with deterministic parameters to accurately identify the most risky element for people, which may either under- or overestimate the risk level (Hu et al., 2017; Yang et al., 2019). Fortunately, Monte Carlo simulation technique, which can define the probability that the risk exceed the guideline threshold value (Tong et al., 2018) and identify priority element of risk control (Ginsberg and Belleggia, 2017), has proved to be one of the most useful approaches for probabilistic risk analysis (Tong et al., 2018; Yang et al., 2019). Therefore, to accurately identify the highlight risky HMs, a probabilistic risk estimation method using Monte Carlo simulation was applied to assess the concentration-oriented and source-oriented health risks caused by soil HMs in this study.

Previous HRA of soil HM pollution was mainly focused on agricultural, mining and smelting area (Arvay et al., 2017; Song et al., 2018; Zhang et al., 2020; Zhou et al., 2018), while few studies have been conducted in urban parks, especially that in large megacity. Shanghai is one of the most populous cities in the world with a population of 24.3 million in 2019 (SMSB, 2020), and its number of urban parks has exceeded 100. However, there is still a lack of study on the public safety of HMs in park soils in this area, even though so many people may be involved.

Therefore, taking a typical megacity (Shanghai) as a case, the main objectives of this study were (1) to explore the pollution characteristics of soil HMs in urban parks, (2) to identify and quantify the potential pollution sources of HMs, (3) to assess the concentration-oriented and source-oriented health risks caused by HMs in park soils.

2. Materials and methods

2.1. Study area and soil sampling

Shanghai (30.7°N- 31.9°N, 120.9°E - 122.2°E) is located at the mouth of the Yangtze River in central eastern coast of China, with an area of 6340.5 km^2. The industrial and agricultural areas are mostly in the rural or suburban areas, while the commercial and residential properties are mostly in the central city. In this study, the design of sampling locations was based on the previous studies (Hung et al., 2018; Jin et al., 2019; Peng et al., 2019). The study area was divided into a sampling grid of 20 km × 20 km, while the central city of Shanghai was further divided into a sampling grid of 4 km × 4 km (Fig. 1). The specific parks selected for soil sampling were as close as practicably possible to the center of each grid.

According to the size of different parks, one to three sampling points were set up in the areas where tourists often gather or pass by. The representative sample of each sampling point is a mixture of five equal weight subsamples of topsoil (0–10 cm). According to the specification of GB/T 36197-2018 issued by the Standardization Administration of China, the 5 subsamples were collected from five locations (Fig. S1). Finally, a total of 204 representative samples were collected from 78 urban parks of the study area. The collected soil samples were kept in polyethylene bags, numbered and marked separately, and then transported to the laboratory. For all samples, the original mass was greater than 1000 g, and the mass after drying and sieving was greater than 500 g.

2.2. Sample analysis

In the laboratory, soil samples were naturally dried at room temperature, sieved to < 0.15 mm, homogenized, digested by microwave

with a typical concentrated acid mixture of HNO_3-HF-$HClO_4$, and kept in amber glass vials before assaying. The concentrations of Cu, Cr, Ni, Zn, Pb, Cd and V were determined by Inductively Coupled Plasma Mass Spectrometry (ICPMS-7900, Thermo Fisher, USA), and the concentrations of As and Hg were measured by Atomic Fluorescence Spectrometer (AFS-8220, Beijing Titan Instruments, China). For Cu, Cr, Ni, Zn, Pb, Cd and V, the analyses and quality assurance/quality control (QA/QC) followed the method of USEPA 6020B (USEPA, 2014b), while As and Hg followed the method of HJ680 (MEP, 2013).

2.3. Data analysis

2.3.1. Evaluation method of pollution levels

To assess the pollution level of individual HMs in soils, two geochemical pollution indices including Geo-accumulation index (I_{geo}) and Enrichment factor (EF) were applied (Kamani et al., 2018):

$$I_{geo} = \log_2\left(\frac{C_i}{1.5 \cdot B_i}\right) \quad (1)$$

$$EF = \frac{(C_i/C_{ref})_{sample}}{(C_i/C_{ref})_{background}} \quad (2)$$

Both I_{geo} and EF are unitless. Where C_i represents the measured concentration of element (mg/kg), B_i denotes the geochemical background of element (mg/kg), C_{ref} is the concentration of reference element (mg/kg), and the coefficient 1.5 is generally used to regulate the anthropogenic impacts (Chen et al., 2019; Muller, 1969). In this study, Al was selected as the normalized reference element since it is one of the largest components in soil. The classification criteria of the I_{geo} and EF were presented in Table S1.

2.3.2. Ecological risk assessment

To assess the overall ecological risks of all HMs considered, the Improved Nemerow index (INI) was developed by Liu et al. (2020). Unlike the index of I_{geo} which can only assess the pollution level of individual elements, the INI (no unit) can use to assess the overall pollution caused by all elements. which is defined as follows:

$$INI = \sqrt{\frac{I_{geo_{max}}^2 + I_{geo_{avg}}^2}{2}} \quad (3)$$

Where $I_{geo_{max}}$ and $I_{geo_{avg}}$ are the maximum value and the mean value of I_{geo} for HMs, respectively. The classification level of INI was given in Table S2.

To assess the potential impact of pollutants on ecosystems, the potential ecological risk (RI) index was developed by Hakanson (1980), which can be used to evaluate the degree of environmental risk caused by all soil HMs (Kamani et al., 2018). The RI can be calculated as follows:

$$RI = \sum E_r^i = \sum T_r^i \times C_f^i = \sum T_r^i C_i / C_b^i \quad (4)$$

Where RI (no unit) is the total potential ecological risk index for all HMs, E_r^i (no unit) is the single ecological risk index for a given element, T_r^i is the toxic response coefficient (no unit), C_f^i (no unit) is the pollution coefficient of element, C_i is the measured concentration of element (mg/kg), and C_b^i is the reference value of element (mg/kg). The values of T_r^i for Cu, Cr, Ni, Zn, Pb, Cd, As, Hg and V were set with 5, 2, 5, 1, 5, 30, 10, 40 and 2, respectively (Hakanson, 1980; Zhuang et al., 2018). The assessment criteria for RI were shown in Table S3.

2.3.3. Source apportionment model

In this study, the PMF model was applied for source apportionment (USEPA, 2014a). The core of the algorithms for PMF model is to minimize the objective function Q, which is calculated as follows (Guan et al., 2018):

$$X_{ij} = \sum_{k=1}^{p} g_{ik} f_{kj} + e_{ij} \quad (5)$$

$$Q = \sum_{i=1}^{n} \sum_{j=1}^{m} \left(\frac{x_{ij} - \sum_{k=1}^{p} g_{ik} f_{kj}}{u_{ij}}\right)^2 \quad (6)$$

$$\text{For } c \le MDL, u_{ij} = \frac{5}{6} MDL \quad (7)$$

$$\text{Else,} \quad u_{ij} = \sqrt{(Errorfraction \times c)^2 + \left(\frac{MDL}{2}\right)^2} \quad (8)$$

Where i, j and k are the number of samples, elements and different sources, respectively. X_{ij} is the concentration of element j in sample i (mg/kg); g_{ik} is the contribution of source k in sample i (mg/kg); f_{kj} is the amount of element j from source k; e_{ij} is the residual; u_{ij} is the uncertainty of element j in sample i; MDL is the species-specific method detection limit; and Error fraction is the percentage of measurement uncertainty.

2.3.4. Probabi listic health risk assessment

The HRA method, recommended by the USEPA (2011), can be used to assess the potential health risks of HMs (Chen et al., 2019). According to the model guidelines, the human health risks caused by various exogenous compounds are divided into two types: Carcinogenic risk (CR) and Non-carcinogenic risk (NCR). Generally, CR is defined as the probability that an individual will develop cancer over a lifetime due to exposure to a particular contaminant or to a mixture of contaminants in the environment (Kamarehie et al., 2019), while NCR is more associated with chronic exposure include genetic and teratogenic effects (USEPA, 1989). Meanwhile, local people are usually grouped into three groups including children, adult males and adult females, and they were separately assessed due to their physiological differences (USEPA, 2011). The Hazard index (HI) represented the accumulative non-carcinogenic risks (Jafari et al., 2019). The Total carcinogenic risk (TCR) was obtained by adding up the potential risks of all individual carcinogenic HMs (Ma et al., 2018). The average daily intake dose (ADD, mg kg^{-1} day^{-1}) estimated the exposures by ingestion, dermal and inhalation absorption pathways, which can be calculated as follows:

$$HI = \sum HQ = \sum \frac{ADD_{ij}}{RfD_{ij}} \quad (9)$$

$$TCR = \sum CR = \sum ADD_{ij} \times SF_{ij} \quad (10)$$

$$ADD_{ingest} = \frac{C \times R_{ingest} \times EF \times ED}{BW \times AT} \times 10^{-6} \quad (11)$$

$$ADD_{dermal} = \frac{C \times SA \times SL \times ABF \times EF \times ED}{BW \times AT} \times 10^{-6} \quad (12)$$

$$ADD_{inhal} = \frac{C \times R_{inhal} \times EF \times ED}{PEF \times BW \times AT} \quad (13)$$

For non-carcinogenic risk, the HI is the sum of the HQ of all HMs. If the values of HI > 1, it indicates that there are potential adverse health effects (MohseniBandpi et al., 2018). For carcinogenic risk, if the values of CR exceed the risk threshold of 1E-04, it indicates human suffers from significant risks of cancer; whereas the values of CR below the acceptable threshold of 1E-06 are generally considered to pose a negligible risk to human health (USEPA, 2009). The detailed explanations of the parameters and the real data for Chinese people that were used in equations are defined in Table S5. The corresponding reference toxicity

Table 1
Statistical summary of soil heavy metal(loid) concentrations (mg/kg) for urban parks in Shanghai.

	Min	Max	Median	Mean	SD	CV/%	Skewness	Kurtosis	ABV	Guide value
Cu	14.3	180.0	34.7	40.4	19.9	49.4	3.3	15.6	26.0	2000.0
Cr	66.7	255.0	108.5	115.3	28.8	25.0	2.1	6.3	68.5	n/a
Ni	21.7	95.1	36.8	37.4	6.5	17.4	4.5	35.8	28.4	150.0
Zn	57.1	396.0	135.5	144.8	52.3	36.1	1.4	2.9	79.9	n/a
Pb	18.3	777.0	34.7	45.0	55.5	123.5	11.4	149.0	24.5	400.0
Cd	0.1	1.5	0.3	0.3	0.2	52.4	3.2	17.0	0.1	20.0
As	3.8	17.8	8.1	8.3	2.3	27.1	1.3	3.1	8.9	20.0
Hg	0.0	2.7	0.1	0.2	0.3	131.4	5.0	31.8	0.1	8.0
V	42.0	121.0	85.0	86.4	11.0	12.7	0.2	1.0	88.3	165.0

Abbreviations: CV, coefficient of variation; ABV, average background value; Guide values were according to GB36600-2018 Soil environmental quality: risk control standard for soil contamination of development land. It recommended screening values which were standard values of soil contaminations. Exceeding the standard may pose risk to human health.

threshold dose (*RfD*, mg/(kg·d)) and slope factors (SF, (kg·d)/mg) values from the literature were shown in Table S6.

Further, to avoid the overestimation or underestimation of risks due to the use of deterministic parameters, the probabilistic risk method (namely Monte Carlo simulation) was applied to assess health risk assessment (Karami et al., 2019). This method can minimize the uncertainties of HRA, by considering the uncertainty of HM concentrations and the variability of specific exposure factors (such as exposure frequency, soil ingestion rate and skin adherence factor).

In summary, the concentration database of HMs fitted a lognormal distribution as an uncertain parameter (Table S4). Meanwhile, the optimal probability distributions for exposure factors were also simulated (Table S5). Then they were incorporated into a risk analysis (Chen et al., 2019; Yang et al., 2019).

Additionally, the result of PMF model was adopted to quantify the contribution of different sources to health risks. Through multiplying the health risk values of individual HMs by the contribution rates of the identified sources, the health risks caused by the different apportioned sources were then obtained (Ma et al., 2018).

2.4. Statistical analysis

All statistical analyses were performed using SPSS v26.0 (IBM, USA). Origin 2018 and ArcGIS10.2 were used for map delineation. Pearson correlation analysis was employed to identify the linear dependence between different variables. PMF model was performed by the EPA PMF v5.0 (USEPA, USA). Before performing PMF model, the dataset was firstly detected, and the outliers were eliminated according to histograms and interquartile ranges, since outliers have a great impact on PMF (Guan et al., 2018; Hu and Cheng, 2016). ArcGIS kriging interpolation was applied to determine the spatial distribution of HMs, which provided new information concerning the potential sources of soil pollution and often used as a confirmation of PMF results (Zhang et al., 2018). In addition, by considering 10,000 iterations with 95% confidence level to obtain stable risk outputs, Monte Carlo simulation was conducted by the software of Crystal Ball v11.1.24 (Oracle, USA) (Karami et al., 2019).

3. Results and discussion

3.1. Characteristics of heavy metal(loid) concentrations

Descriptive statistics for the HMs in soil samples were presented in Table 1, including the items of min, max, median, mean, standard deviation, coefficient of variation (CV), skewness and kurtosis. Additionally, the physical and chemical properties of soil samples were shown in Table S7. The major components of soil include Al, Ca, K, Mg and Na, and their mean values were 6.23%, 1.99%, 1.52%, 1.12% and 1.07%, respectively.

Comparing the concentrations of HMs with the national guide values of china (MEE, 2018), the maximum concentrations of all HMs except Pb were lower than their corresponding soil quality standard (Table 1). Statistical summary of concentrations of HMs in topsoil concerning global urban parks given in literature were shown in Table S8. Relatively, the levels of concentrations for HMs in park soils of the study area were slightly higher than those in other areas, such as USA, Korea, Brazil and most other Chinese cities.

The mean concentrations of Zn, Cr, V, Pb, Cu, Ni, As, Cd and Hg were 144.8, 115.3, 86.4, 45.0, 40.4, 37.4, 8.3, 0.3 and 0.2 mg/kg, respectively (Table 1). Except for As and V, the mean concentrations for other HMs in park soils were greater than their local average background values (ABVs) (CNEMC, 1990). In particular, the mean concentrations of Hg, Cd and Pb were 2.72, 2.34 and 1.84 times greater than their corresponding local ABVs, respectively (Fig. S2). In addition, the proportions of Cd, Pb and Hg exceeding the background values in all samples were 99.02%, 92.16% and 83.33% respectively, indicating that

Table 2
Class distribution for contamination assessment of heavy metal(loid)s in park soils from Shanghai by Geo-accumulation index (I_{geo}) and Enrichment factor (EF).

Class distribution (%)	Cu	Cr	Ni	Zn	Pb	Cd	As	Hg	V
(a) Geo-accumulation index (I_{geo})									
UP	63.24	37.75	91.67	38.24	57.84	18.63	97.06	36.27	100.00
UP to MP	32.35	59.31	7.84	53.92	33.82	61.76	2.94	41.18	0.00
MP	3.92	2.94	0.49	7.84	7.35	17.65	0.00	17.16	0.00
MP to HP	0.49	0.00	0.00	0.00	0.49	1.96	0.00	2.45	0.00
HP	0.00	0.00	0.00	0.00	0.00	0.00	0.00	2.45	0.00
HP to EP	0.00	0.00	0.00	0.00	0.49	0.00	0.00	0.49	0.00
EP	0.00	0.00	0.00	0.00	0.00	0.00	0.00	0.00	0.00
(b) Enrichment factor (EF)									
Minimal enrichment	75.49	68.63	99.51	51.96	66.67	36.27	97.06	46.57	97.55
Moderate enrichment	22.06	30.88	0.49	46.57	29.90	53.92	2.45	42.16	2.45
Significant enrichment	2.45	0.49	0.00	1.47	2.94	9.80	0.49	9.31	0.00
Very high enrichment	0.00	0.00	0.00	0.00	0.49	0.00	0.00	1.96	0.00
Extremely high enrichment	0.00	0.00	0.00	0.00	0.00	0.00	0.00	0.00	0.00

Abbreviations: UP, Unpolluted; MP, Moderately polluted, HP: Heavily polluted, EP: Extremely polluted. I_{geo} and EF are unitless.

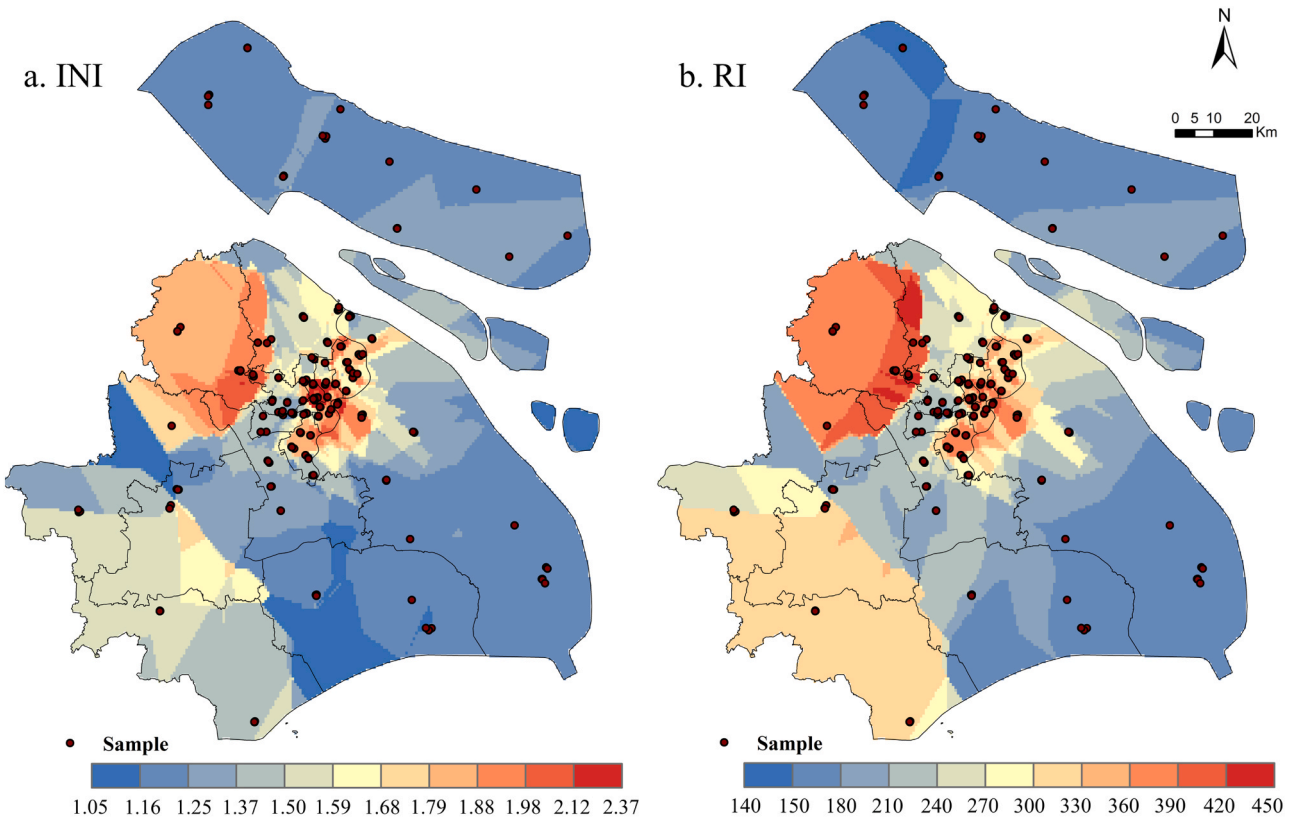

Fig. 2. Contamination assessment of heavy metal(loid)s in park soils by using Improved Nemerow index (INI) and Potential ecological risk index (RI).

Hg, Cd and Pb may be the main enriched pollutants in park soils. In term of the classification criteria of the degree of variation (Hu et al., 2011), Hg, Pb, Cd, Cu and Zn showed relatively high spatial variation (CV > 30%), especially Hg and Pb with the variation coefficients of 131.36% and 123.46%, respectively. The high variations may be due to the high concentrations in some sampling points, indicating that both Hg and Pb may be resulted from point source pollution. The relatively high kurtosis of the Pb distribution indicated the existence of unusually high values, which might be related to the anthropogenic emissions (Huang et al., 2020; Jin et al., 2019).

3.2. *Environmental risks of heavy metal(loid) pollution in park soils*

To identify the impact of anthropogenic activities on the level of HM pollution in park soils, I_{geo} and EF were calculated (Table 2). In all samples, 7.84%, 8.33%, 19.61% and 22.55% of Zn, Pb, Cd and Hg had the I_{geo} values at the level of "moderately polluted" (MP) or higher, respectively. Similarly, the EF results revealed that the average EF values of Zn (2.11), Pb (2.12), Cd (2.77) and Hg (3.15) in soils were greater than 2, implying that anthropogenic activities may play an important role in the high accumulation of these HMs in park soils (Table S1).

As a whole, the parks soils in the study area were largely polluted by Cu, Cr, Zn, Pb, Cd and Hg with varying degrees. Relatively, Hg was considered to be the most polluted pollutant with high concentration characteristic and I_{geo} value (Tables 1 and 2a), indicating that Hg pollution in these parks has been seriously affected by anthropogenic sources (Chen et al., 2019). According to EF results, the 53.43% EF values of Hg were at moderate enrichment to very high enrichment level (Table 2b), which indicated that Hg in most soils were at a serious pollution level. In addition to Hg, the elements of Cd and Pb were also considered as two other serious pollutants in park soils (Tables 1 and 2a), with 11.27% Hg, 9.8% Cd and 3.43% Pb of EF values in soils exceeded 5 showing significant or higher enrichment. In short, the serious pollution levels of Hg, Cd and Pb in park soils may be largely related to anthropogenic activities, such as traffic emissions, industrial production, and agricultural activities, etc.(Huang et al., 2015; Wang et al., 2019b).

The results of INI demonstrated that most soil samples (98.04%) had the ecological risks of potential HM contamination (> class 0), and 8.82% of them even reached the level of "moderately to extremely contaminated" (Fig. S3 and Table S3). It indicated that the overall ecological risk of soil HMs in urban parks was generally acceptable, but some needed environmental quality protection or ecological restoration.

The RI values of HMs in park soils presented a moderate risk, with a mean value of 268.7 (Table S3). Relatively, due to the high toxic response factor and/or high enrichment (Chen et al., 2019), Hg, Cd and Pb posed higher ecological risks than the other HMs. Approximately 88.2% of Cd samples, 83.3% of Hg samples, and 0.5% of Pb samples were at the "moderate risk" level or higher (Table S9). Among them, 4.4% of Hg samples showing a "very-high risk" level, which was higher than that of Cd (0.5%). It indicated that Hg was the major pollutant causing ecological risk in park soils, followed by Cd and Pb.

As shown in Fig. 2, the spatial distribution of HMs in park soils was significantly different depending on the location of the park studied. The INI and RI values of soil HMs in central city and west suburban area of the study area were higher than those in other regions. The central city area (Fig. 1), in which residential and commercial properties were mainly located, had the densest population, the densest historical sites, the busiest urban traffic, and the most tourists (Li et al., 2011). While the western area was located in the suburban or rural areas (Fig. 1), with the highest concentration of agricultural areas and industrial facilities. Jin et al. (2019) and Liu et al. (2020) also reported the similar result that the HM concentrations in park soils were higher in the central urban areas and the agricultural and industrial areas, indicating a necessity to strengthen the protection of soil environmental quality in these areas.

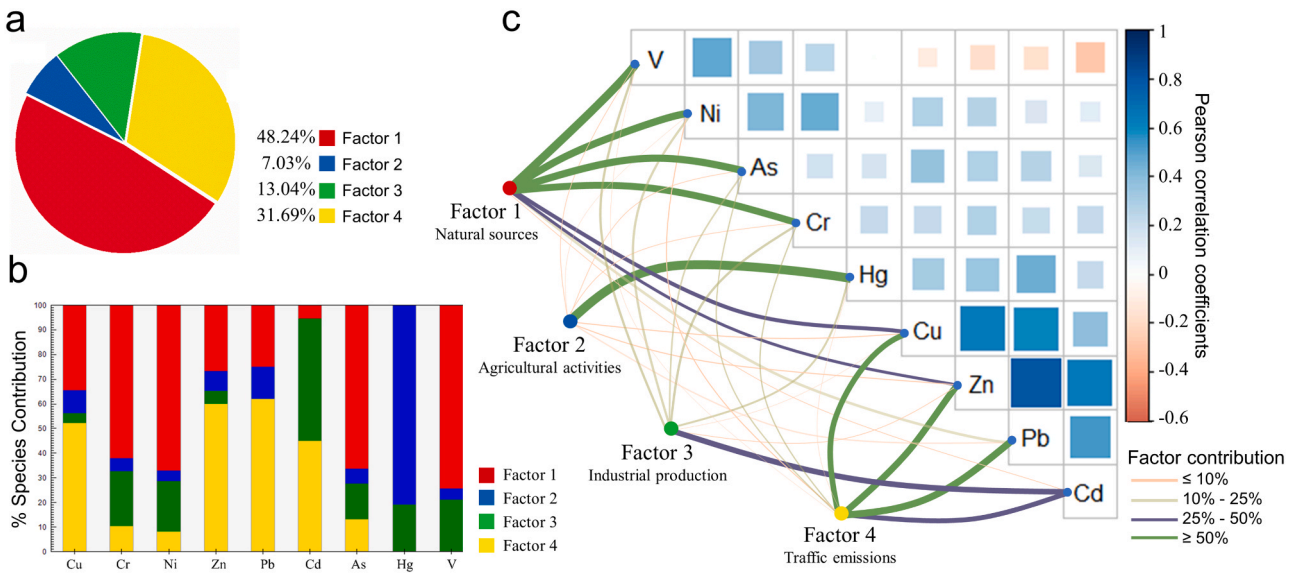

Fig. 3. Source apportionment of heavy metal(loid)s (HMs) in park soils of the study area. a) The percentage of contribution for each Factor by positive matrix factorization (PMF) model. b) Factor profiles of HMs in soils of 78 parks derived from PMF model. c) Identify the correlations between HMs by combining Pearson correlation analysis and PMF model. Pairwise comparisons of heavy metal(loid)s were shown with a color gradient denoting correlation coefficient. Factor contribution from PMF was related to each heavy metal(loid). Edge width corresponded to the values of factor loading in proportion, and edge colors denoted the ranges of factor loadings. (For interpretation of the references to colour in this figure legend, the reader is referred to the web version of this article.)

3.3. Source apportionment of heavy metal(loid)s

To effectively apportion the natural and anthropogenic sources of HMs, Pearson correlation analysis was used to initially identify the correlations between the concentrations of HMs studied. Then, PMF model was applied to apportion and quantify the potential sources of HMs (Fig. 3a–b). In addition, to verify the results of source apportionment, this study correlated the factor contributions from PMF model with the Pearson correlation coefficients of HMs (Fig. 3c). In the PMF model, a minimum objective function Q was applied to ensure residual matrix (Chen et al., 2019; Guan et al., 2018), and then the appropriate number of factors was determined to be four. The signal-to-noise ratios (S/N) of all HMs were defined as "strong". The fitting coefficients (r^2) between the observed concentrations and predicted concentrations were presented in Fig. S4. The detailed Factors profiles and contributions of individual HMs by PMF model were shown in Figs. S5–S6.

Strong correlations ($r > 0.6$) were observed in the pairwise comparisons of soil HMs (Fig. 3c), which indicated a potential common source (Jin et al., 2019). PMF model extracted four factors (named as Factor 1, Factor 2, Factor 3, and Factor 4, respectively), and their contribution percentages were presented in Fig. 3a. The PMF results indicated that Factor 1 mainly loaded on V, As, Ni and Cr; Factor 2 was weighted heavily on Hg; Factor 3 was characterized by Cd; and Factor 4 was dominated by Pb, Zn, Cu and Cd (Fig. 3b). In addition, geographical statistical analysis was also used to intuitively reflect the local situation in this study, which has proved an effective method to determine pollution hotspots and explore their sources (Zhang et al., 2018). As a confirmation of source apportionment, the spatial distributions of HM concentrations by GIS methods were presented in Fig. S7.

Factor 1, which accounted for 48.24% of the contribution rate (Fig. 3a), had the strongest correlation with V, As, Ni and Cr in park soils (Fig. 3c). Generally, these elements are related to soil parent materials of lithogenic origin. The source of V and As could be recognized as natural background because their average concentrations in soils were both lower than their corresponding local ABVs (Table 1). Meanwhile, Ni and Cr might also be associated with natural sources, since both of them have been confirmed to be widely present in the pedogenic process and soil parent materials (Jin et al., 2019; Zhang et al., 2018). In addition, the spatial analysis of V, As and Ni did not exhibit obvious point source distribution (Fig. S7). Hence, Factor 1 might be interpreted as natural sources.

Factor 2 with a contribution rate of 7.03% (Fig. 3a) was mostly related to Hg (Fig. 3c). As discussed above, Hg was significantly enriched in park soils, and had the highest ecological risk and pollution level according to the analysis results of I_{geo}, EF, and RI, indicating that Hg was originated from anthropogenic sources. The research of Liu et al. (2020) showed that 80% of man-made Hg sources enter the atmosphere in the form of elemental vapor, which are associated with exhaust emissions, fuel combustion and waste incineration. Dong et al. (2017) and Giersz et al. (2017) also confirmed that the Hg contamination in soils mainly comes from the application of Hg-containing pesticides and sludge fertilizers due to its strong volatility and migration. Besides, the spatial distribution analysis (Fig. S7) showed that Hg was more accumulated in western suburban parks, which may be related to the use of pesticides and fertilizers with high concentrations of Hg in many farmlands before being converted into parks. Therefore, Factor 2 might be related to agricultural activities.

Factor 3, with a contribution rate of 13.04% (Fig. 3a), was mainly characterized by Cd (Fig. 3c). Liu et al. (2020) found that industrial output and distance from the city center were the main factors for Cd contamination. Khan et al. (2016) also showed that copious amounts of Cd were released into the surrounding environment due to fossil fuel consumption, metal smelting and waste incineration. Shanghai is one of the most developed regions in China, with considerable centuries-old parks, which leads to the long-term enrichment of HMs in soils. The areas with high Cd concentrations were mainly distributed in the central city area with the largest number of visitors (Fig. S7). According to the field investigation, solid wastes such as cigarette butts discarded by tourists are the most common forms of litter in parks and represent potential point sources for soil pollution, especially in parks of the central city area. Previous studies have confirmed that considerable HMs including Cd may enter the environment from discarded cigarette litter every year (Dobaradaran et al., 2017; Kurmus and Mohajerani, 2020) and battery (Jiang et al., 2020). Thus, Factor 3 might be allocated to industrial production.

Factor 4 with a contribution rate of 31.69% (Fig. 3a) was mainly loaded on Pb, Zn, Cu and Cd (Fig. 3c). The parks with high concentrations of these HMs were more accumulated in the central city (Fig. S7),

Table 3
Summary statistics for non-carcinogenic and carcinogenic health risk range based on Monte Carlo simulation.

Risk	HMs	Mean (median)			SD			95% CI		
		Children	Adult males	Adult females	Children	Adult males	Adult females	Children	Adult males	Adult females
HQ	Cu	3.1E-03 (2.8E-03)	3.5E-04 (3.1E-04)	4.0E-04 (3.6E-04)	1.4E-03	2.0E-04	2.3E-04	(7.0E-04, 1.7E-02)	(2.6E-05, 2.3E-03)	(3.4E-05, 3.3E-03)
	Cr	1.2E-01 (1.1E-01)	1.4E-02 (1.3E-02)	1.6E-02 (1.5E-02)	3.8E-02	5.9E-03	6.9E-03	(3.7E-02, 3.4E-01)	(2.0E-03, 5.8E-02)	(1.6E-03, 5.9E-02)
	Ni	5.7E-03 (5.5E-03)	6.4E-04 (6.3E-04)	7.5E-04 (7.3E-04)	1.5E-03	2.6E-04	3.0E-04	(1.9E-03, 1.5E-02)	(7.1E-05, 1.8E-03)	(8.6E-05, 2.2E-03)
	Zn	1.5E-03 (1.4E-03)	1.7E-04 (1.5E-04)	2.0E-04 (1.8E-04)	6.2E-04	8.7E-05	1.0E-04	(2.9E-04, 6.6E-03)	(1.6E-05, 8.0E-04)	(1.5E-05, 1.1E-03)
	Pb	3.7E-02 (3.1E-02)	4.2E-03 (3.5E-03)	4.9E-03 (4.1E-03)	2.3E-02	2.9E-03	3.5E-03	(8.0E-03, 3.5E-01)	(2.8E-04, 5.3E-02)	(2.8E-04, 5.9E-02)
	Cd	9.0E-04 (7.8E-04)	1.1E-04 (9.1E-05)	1.2E-04 (1.1E-04)	4.9E-04	6.7E-05	7.9E-05	(2.0E-04, 6.8E-03)	(1.2E-05, 9.5E-04)	(1.1E-05, 1.0E-03)
	As	8.3E-02 (7.9E-02)	9.6E-03 (9.0E-03)	1.1E-02 (1.1E-02)	2.9E-02	4.5E-03	5.3E-03	(2.7E-02, 2.4E-01)	(7.7E-04, 4.0E-02)	(9.1E-04, 4.4E-02)
	Hg	2.1E-03 (1.5E-03)	2.4E-04 (1.6E-04)	2.8E-04 (1.9E-04)	2.1E-03	2.6E-04	2.9E-04	(1.4E-04, 3.3E-02)	(7.3E-06, 5.6E-03)	(6.9E-06, 4.1E-03)
	V	3.8E-02 (3.7E-02)	4.3E-03 (4.2E-03)	5.0E-03 (4.9E-03)	9.9E-03	1.7E-03	2.0E-03	(1.4E-02, 8.6E-02)	(4.6E-04, 1.2E-02)	(5.4E-04, 1.4E-02)
HI	Total	2.9E-01 (2.8E-01)	3.3E-02 (3.2E-02)	3.9E-02 (3.8E-02)	7.9E-02	1.3E-02	1.6E-02	(1.1E-01, 7.2E-01)	(4.1E-03, 9.4E-02)	(4.7E-03, 1.1E-01)
CR	Cr	3.3E-07 (3.1E-07)	3.9E-07 (3.8E-07)	3.8E-07 (3.6E-07)	1.0E-07	1.1E-07	1.1E-07	(1.1E-07, 1.1E-06)	(1.5E-07, 1.2E-06)	(1.3E-07, 1.1E-06)
	Ni	4.7E-10 (4.7E-10)	1.8E-09 (1.8E-09)	1.6E-09 (1.5E-09)	9.5E-11	3.6E-10	3.2E-10	(2.2E-10, 9.8E-10)	(7.5E-10, 3.6E-09)	(6.8E-10, 3.2E-09)
	Pb	**9.5E-08** (7.9E-08)	**4.3E-08** (3.6E-08)	**5.0E-08** (4.2E-08)	5.7E-08	3.0E-08	3.4E-08	(2.3E-08, 8.0E-07)	(2.9E-09, 4.7E-07)	(4.0E-09, 5.4E-07)
	Cd	4.6E-07 (4.0E-07)	2.1E-07 (1.8E-07)	2.5E-07 (2.1E-07)	2.5E-07	1.3E-07	1.6E-07	(1.0E-07, 4.0E-06)	(1.6E-08, 1.5E-06)	(1.5E-08, 1.8E-06)
	As	**3.3E-06** (3.1E-06)	**1.5E-06** (1.4E-06)	**1.7E-06** (1.6E-06)	1.2E-06	7.0E-07	8.0E-07	(7.3E-07, 1.2E-05)	(8.7E-08, 6.6E-06)	(1.6E-07, 6.1E-06)
TCR	Total	**4.2E-06** (4.0E-06)	**2.1E-06** (2.0E-06)	**2.4E-06** (2.3E-06)	1.3E-06	8.4E-07	9.9E-07	(1.2E-06, 1.2E-05)	(3.6E-07, 6.9E-06)	(3.9E-07, 8.3E-06)

Abbreviations: SD, Standard deviation; CI, Confidential interval; HQ, Hazard quotient of each HMs; HI, Hazard index posed by multiple HMs; CR, Carcinogenic risk of each HMs; TCR, Total carcinogenic risks posed by multiple HMs.

and the concentrations decreased with the distance from the city center. The closer to the city center reflected greater traffic volume (Liu et al., 2020). In particular, it was known that Pb, Cu and Zn pollutants in soils usually originate from engine wear, leaded gasoline, braking and other traffic sources (Dao et al., 2014; Du et al., 2019; Zhang, 2005). Besides, Cd was a component of tires and lubricants, and Zn was a constituent of tire hardeners, bitumen and exhaust emissions (Li et al., 2001). This might reflect the impact of traffic related activities on these HMs accumulation. Roadside soil polluted by exhaust emissions or vehicle tire wear might enter the park in the form of dust (Jin et al., 2019). Since these HMs were rarely degraded by self-migration or microbial degradation, they can stay in soils for a long time, causing their accumulation in park soils. Therefore, Factor 4 might be assigned to traffic emissions.

3.4. Probabilistic health risks assessment

3.4.1. Concentration-oriented health risk assessment

By using Monte Carlo simulation, the NCR and CR of all populations (including children, adult males, and adult females) exposed to HMs in park soils through three different ways were assessed, and the results were presented in Table 3.

For all populations, the NCR was negligible. The probability distribution of calculated Hazard index (HI) and Hazard quotient (HQ) were shown in Fig. 4. The mean HI values for all populations were below the USEPA's guideline value of 1 (Fig. 4a), indicating no potential non-carcinogenic risks. Compared with adults, children suffered from a greater accumulative non-carcinogenic risk, and the mean values of HI decreased in the following order: children > adult females > adult males (Fig. 4a). Additionally, the HQ values of all HMs for children, adult females and males were less than 1, indicating that these HMs studied barely pose a non-carcinogenic risk to human health. The basic trend of mean HQ values for all groups was Cr > As > V > Pb > Ni > Cu > Hg > Zn > Cd (Fig. 4b–j).

According to the probability distribution shown in Fig. 5a, the TCR of five HMs studied cannot be negligible, while the CR values for individual HMs were different. The mean values of TCR values for children, adult females and males were 4.2E-06, 2.4E-06 and 2.1E-06 respectively, which all exceeded the acceptable threshold of 1E-06. The relatively high exceedance was found in Fig. S8, indicating a high risk of causing cancer (Gu et al., 2017; Rahman et al., 2019). Besides, the mean TCR value for children was 4.2E-06 with the 95% confidential interval of 1.2E-06 to 1.2E-05 (Fig. 5a and Table 3), which was about four times greater than the acceptable threshold of 1E-06. Meanwhile, nearly 100.0%, 95.2%, 93.5% of TCR values surpassed 1E-06 for children, adult females and adult males, respectively, which indicated a non-negligible carcinogenic risk. According to Fig. 5b–e, As was confirmed as the dominant element of carcinogenic risk by comparing the largest mean CR value. Among all populations, the mean CR values for As exceeded the acceptable threshold of 1E-06. Especially, the CR of As for children exceeded the risk threshold of 1E-06 even at the 5th percentile (Table S10). In addition, according to their percentage of risk values exceeding the threshold of 1E-06 (Fig. S8), it was found that As showed the highest risk for all populations, which may lead to lung, skin, kidney and liver cancer (Cogliano et al., 2011). Therefore, the risk assessment undertaken in urban parks of China's megacities should pay closer attention to HMs exposure for children, especially to As.

3.4.2. Source-oriented health risk assessment

To investigate the health risks caused by different pollution sources of HMs, a comprehensive method (named as PMF-HRA) was developed

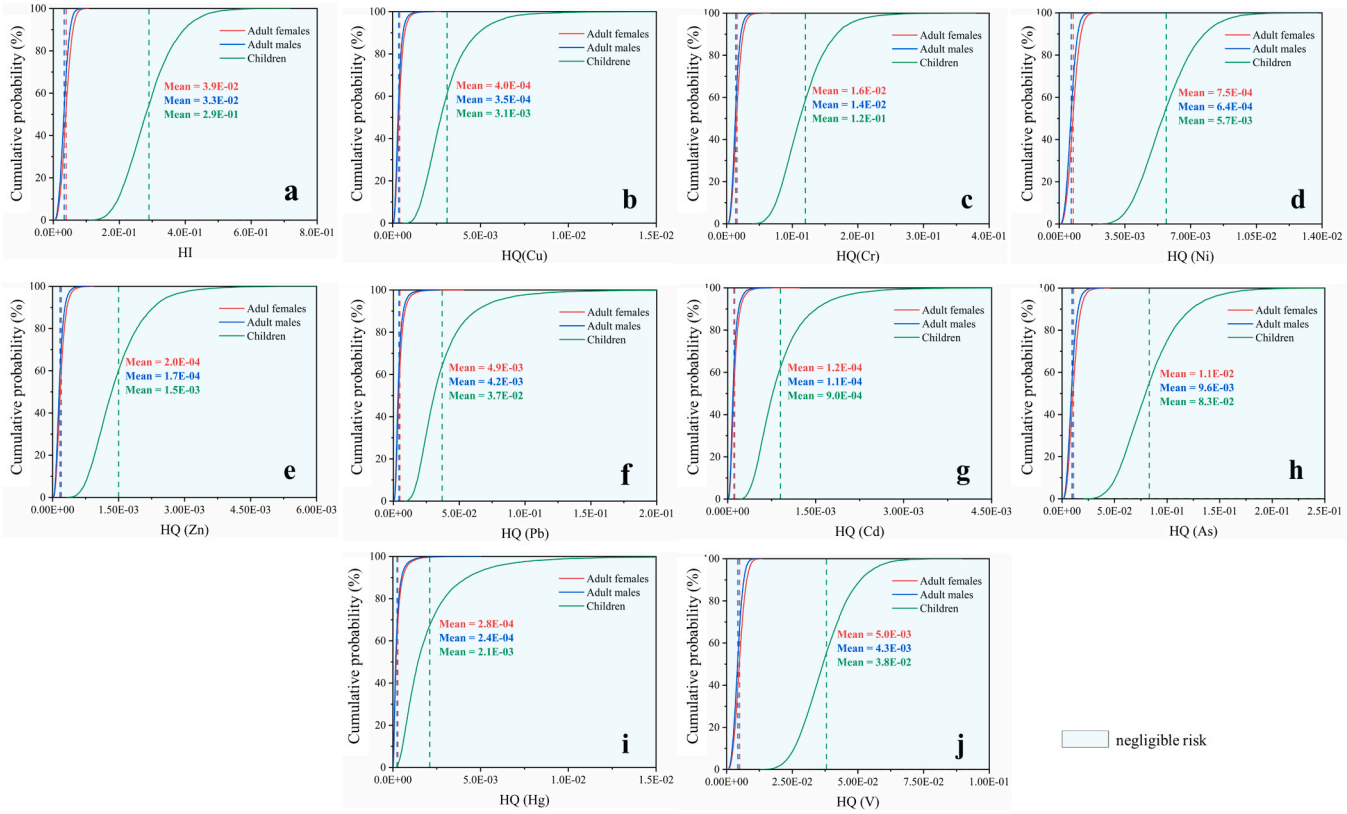

Fig. 4. Probability distribution for a) Hazard index (HI); and for Hazard quotient (HQ) of b) Cu, c) Cr, d) Ni, e) Zn, f) Pb, g) Cd, h) As, i) Hg, and j) V. The red, blue or green vertical dashed lines represented the mean values for adult females, adult males, and children, respectively. (For interpretation of the references to colour in this figure legend, the reader is referred to the web version of this article.)

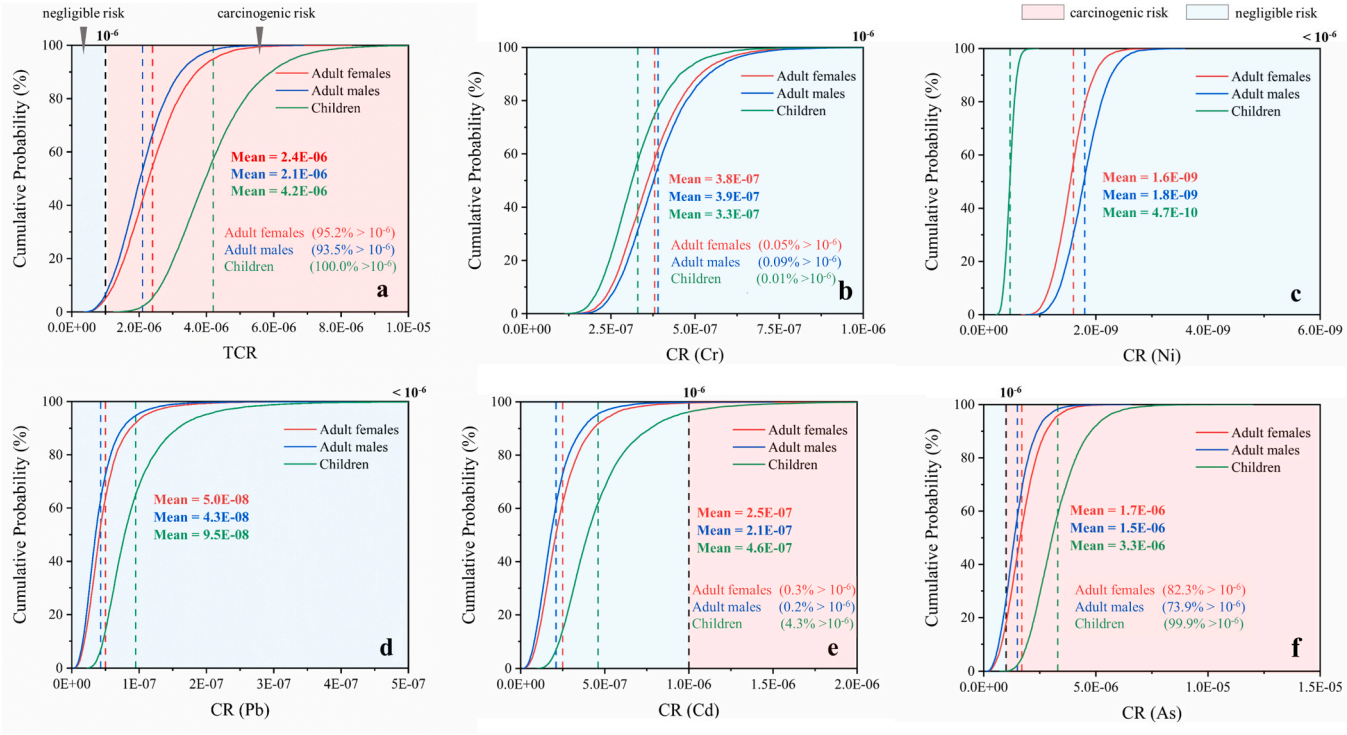

Fig. 5. Probability distribution and the percentage surpassed 1E-06 for a) Total carcinogenic risk (TCR) and Carcinogenic risk (CR) index of b) Cr, c) Ni, d) Pb, e) Cd and f) As. The red, blue or green vertical dashed lines represented the mean values while the black represented the acceptable threshold (1E-06). (For interpretation of the references to colour in this figure legend, the reader is referred to the web version of this article.)

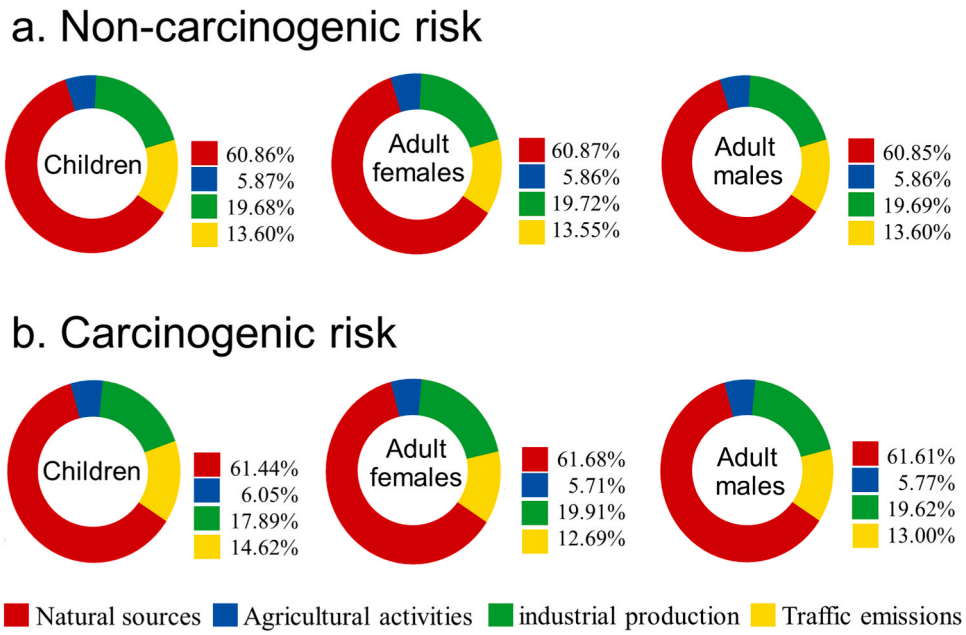

Fig. 6. Comparison of health risks caused by different pollution sources of heavy metal(loid)s. a) Non-carcinogenic risk and b) Carcinogenic risk for children, adult females, and adult males, respectively.

on the basis of the PMF model couple with the HRA model. Based on the results of source apportionment using PMF model, the contribution rates of different sources were further used to assess the NCR and CR. As shown in Fig. 6, the contribution rates of different pollution sources to health risks were similar among children, adult females and males, which was consistent with the study results of Ma et al. 2018. Among the four pollution sources of HMs, the industrial and traffic sources were always estimated to be the most important anthropogenic sources of health risks for all three groups (Fig. 6). It indicated that the industrial and traffic sources might pose a significant impact on human health risks, and because Cd, Pb and Zn were loaded most on these two factors (Fig. 3b), they were identified as the priority contaminants for further risk control.

The sampling sites with high Cd, Pb and Zn risk were mainly in the central city (Fig. S7) with a high density of population. Moreover, among all populations, children were exceptionally more sensitive than adults to exposure of HMs in soils, as reflected by the higher mean HI and TCR values for children than that for adults, which is mainly attributed to their hand-to-mouth behavior (Ma et al., 2018; Qu et al., 2012; Yang et al., 2019). Therefore, the prevention and control of health risks undertaken in urban parks of China's megacities should pay closer attention to HMs exposure, especially for children.

Quantifying the contribution of different HM sources to health risks can help develop risk mitigation strategies by adopting a prioritization of actions in urban parks, which could best minimize the risks for people. Our results generally emphasized that the risks to human health caused by exposure to HMs in park soils cannot be ignored, and special consideration should be given to further risk control. Whereas, long-term health impact will be profound for people if remedial actions are not undertaken.

4. Conclusions

In conclusion, taking a megacity with a large population as a case, we have conducted the research on characteristics, sources and health risks of HMs in urban park soils. Results revealed that the Hg, Cd and Pb were the most serious pollutants and showed higher ecological risks than the other HMs. The concentration-oriented and source-oriented health risks were assessed by using Monte Carlo simulation coupled with PMF model, and the results showed that the NCR of HMs for all populations were acceptable, while the TCR stayed at a relatively high level. The source analysis was carried out based on the combination of the PMF model and Correlation analysis, which improved the accuracy of source identification and effectively quantified the contribution of pollution sources. In addition, a probabilistic risk estimation method by using Monte Carlo simulation was used to assess health risks, which can accurately identify the highlight risky HMs for further risk control.

However, in this study, the HRA was performed on the basis of the existing monitoring data of HM concentrations. While the physical and chemical properties of soils (such soil type, particle size, soil permeability, and pH, etc.) have been confirmed to have a significant impact on the concentration distribution of HMs (Gasiorek et al., 2017; Gu et al., 2016; Ribeiro et al., 2013; Shepard, 1954; Zarezadeh et al., 2017). Therefore, to provide more scientific support for the prevention and control of HM pollution, more investigations on the relationship between the physical and chemical properties of soils and the status of HM pollution are needed to reduce the assessment bias.

CRediT authorship contribution statement

Jingling Huang: Data curation, Formal analysis, Validation, Visualization, Software, Writing - original draft, Writing - review &editing, Project administration. **Yuying Wu:** Methodology. **Jiaxun Sun**: Investigation. **Xiao Li**: Supervision. **Xiaolei Geng**: Conceptualization. **Menglu Zhao:** Validation. **Ting Sun:** Resources. **Zhengqiu Fan**: Funding acquisition, Writing - review & editing.

Declaration of Competing Interest

The authors declare that they have no known competing financial interests or personal relationships that could have appeared to influence the work reported in this paper.

Acknowledgements

This work was supported by the Guangdong Provincial Key Laboratory of Fishery Ecology and Environment (No. FEEL-2017); and the National Key Research and Development Program of China (No.

2016YFC0502705).

Appendix A. Supporting information

Supplementary data associated with this article can be found in the online version at doi:10.1016/j.jhazmat.2021.125629.

References

Arvay, J., Demkova, L., Hauptvogl, M., Michalko, M., Bajcan, D., Stanovic, R., et al., 2017. Assessment of environmental and health risks in former polymetallic ore mining and smelting area, Slovakia: spatial distribution and accumulation of mercury in four different ecosystems. Ecotoxicol. Environ. Safe 144, 236–244.

Brtnicky, M., Pecina, V., Hladky, J., Radziemska, M., Koudelkova, Z., Klimanek, M., et al., 2019. Assessment of phytotoxicity, environmental and health risks of historical urban park soils. Chemosphere 220, 678–686.

Chen, R., Chen, H., Song, L., Yao, Z., Meng, F., Teng, Y., 2019. Characterization and source apportionment of heavy metals in the sediments of Lake Tai (China) and its surrounding soils. Sci. Total Environ. 694, 445–486.

CNEMC, 1990. The Background Values of Chinese Soil. Environmental Science Press of China, Beijing. China National Environmental Monitoring Centre.

Cogliano, V.J., Baan, R., Straif, K., Grosse, Y., Lauby-Secretan, B., El Ghissassi, F., et al., 2011. Preventable exposures associated with human cancers. J. Natl. Cancer Inst. 103, 1827–1839.

Dao, L., Morrison, L., Zhang, H., Zhang, C., 2014. Influences of traffic on Pb, Cu and Zn concentrations in roadside soils of an urban park in Dublin, Ireland. Environ. Geochem. Health 36, 333–343.

Davis, H.T., Marjorie Aelion, C., McDermott, S., Lawson, A.B., 2009. Identifying natural and anthropogenic sources of metals in urban and rural soils using GIS-based data, PCA, and spatial interpolation. Environ. Pollut. Vol.157, 2378–2385.

Dobaradaran, S., Nabipour, I., Saeedi, R., Ostovar, A., Khorsand, M., Khajeahmadi, N., et al., 2017. Association of metals (Cd, Fe, As, Ni, Cu, Zn and Mn) with cigarette butts in northern part of the Persian Gulf. Tob. Control 26, 461–463.

Dong, H., Lin, Z., Wan, X., 2017. Risk assessment for the mercury polluted site near a pesticide plant in Changsha, Hunan, China. Chemosphere 169, 333–341.

Du, X., Zhu, Y., Han, Q., Yu, Z., 2019. The influence of traffic density on heavy metals distribution in urban road runoff in Beijing. China Environ. Sci. Pollut. Res. 26, 886–895.

Gasiorek, M., Kowalska, J., Mazurek, R., Pajak, M., 2017. Comprehensive assessment of heavy metal pollution in topsoil of historical urban park on an example of the Planty Park in Krakow (Poland). Chemosphere 179, 148–158.

Giersz, J., Bartosiak, M., Jankowski, K., 2017. Sensitive determination of Hg together with Mn, Fe, Cu by combined photochemical vapor generation and pneumatic nebulization in the programmable temperature spray chamber and inductively coupled plasma optical emission spectrometry. Talanta 167, 279–285.

Ginsberg, G.L., Belleggia, G., 2017. Use of Monte Carlo analysis in a risk-based prioritization of toxic constituents in house dust. Environ. Int. 109, 101–113.

Gu, Y.G., Wang, X.N., Lin, Q., Du, F.Y., Ning, J.J., Wang, L.G., Li, Y.F., 2016. Fuzzy comprehensive assessment of heavy metals and Pb isotopic signature in surface sediments from a bay under serious anthropogenic influences: Daya Bay. China Ecotoxicol. Environ. Safe. 126, 38–44.

Gu, Y.G., Lin, Q., Gao, Y.P., 2017. Metals in exposed-lawn soils from 18 urban parks and its human health implications in southern China's largest city, Guangzhou. J. Clean. Prod. 163, 164–171.

Guan, Q.Y., Wang, F.F., Xu, C.Q., Pan, N.H., Lin, J.K., Zhao, R., et al., 2018. Source apportionment of heavy metals in agricultural soil based on PMF: a case study in Hexi Corridor, northwest China. Chemosphere 193, 189–197.

Hakanson, L., 1980. An ecological risk index for aquatic pollution control–a sedimentological approach. Water Res. 14, 975–1001.

Hou, D., Li, F., 2017. Complexities surrounding China's soil action plan. Land Degrad. Dev. 28, 2315–2320.

Houston, M.C., 2012. The role of mercury and cadmium in cardiovascular disease, hypertension, and stroke. Met. Ion. Stroke 767–782.

Hu, B.F., Jia, X.L., Hu, J., Xu, D.Y., Xia, F., Li, Y., 2017. Assessment of Heavy Metal Pollution and Health Risks in the Soil-Plant-Human System in the Yangtze River Delta, China. Int. J. Environ. Res. Public Health 14, 1660–4601.

Hu, X., Zhang, Y., Luo, J., Wang, T., Lian, H., Ding, Z., 2011. Bioaccessibility and health risk of arsenic, mercury and other metals in urban street dusts from a mega-city, Nanjing, China. Environ. Pollut. 159, 1215–1221.

Hu, Y., Cheng, H., 2016. A method for apportionment of natural and anthropogenic contributions to heavy metal loadings in the surface soils across large-scale regions. Environ. Pollut. 214, 400–409.

Huang, J.H., Guo, S.T., Zeng, G.M., Li, F., Gu, Y.L., Shi, Y.H., et al., 2018. A new exploration of health risk assessment quantification from sources of soil heavy metals under different land use. Environ. Pollut. 243, 49–58.

Huang, Y., Li, T.Q., Wu, C.X., He, Z.L., Japenga, J., Deng, M., et al., 2015. An integrated approach to assess heavy metal source apportionment in pen-urban agricultural soils. J. Hazard. Mater. 299, 540–549.

Huang, Y., Dang, F., Li, M., Zhou, D., Song, Y., Wang, J., 2020. Environmental and human health risks from metal exposures nearby a Pb-Zn-Ag mine, China. Sci. Total Environ. 698.

Hung, W.C., Hernandez-Cira, M., Jimenez, K., Elston, I., Jay, J.A., 2018. Preliminary assessment of lead concentrations in topsoil of 100 parks in Los Angeles. Calif. Appl. Geochem. Vol.99, 13–21.

Jafari, A., Ghaderpoori, M., Kamarehi, B., Abdipour, H., 2019. Soil pollution evaluation and health risk assessment of heavy metals around Douroud cement factory. Iran. Environ. Earth Sci. 78, 250.

Jiang, Y., Ma, J., Ruan, X., Chen, X., 2020. Compound health risk assessment of cumulative heavy metal exposure: a case study of a village near a battery factory in Henan Province. China Environ. Sci. Proc. Imp. 22, 1408–1422.

Jin, Y.L., O'Connor, D., Ok, Y.S., Tsang, D.C.W., Liu, A., Hou, D.Y., 2019. Assessment of sources of heavy metals in soil and dust at children's playgrounds in Beijing using GIS and multivariate statistical analysis. Environ. Int. 124, 320–328.

Kamani, H., Mirzaei, N., Ghaderpoori, M., Bazrafshan, E., Rezaei, S., Mahvi, A.H., 2018. Concentration and ecological risk of heavy metal in street dusts of Eslamshahr, Iran. Hum. Ecol. Risk Assess. 24, 961–970.

Kamarehie, B., Jafari, A., Zarei, A., Fakhri, Y., Ghaderpoori, M., Alinejad, A., 2019. Non-carcinogenic health risk assessment of nitrate in bottled drinking waters sold in Iranian markets: a Monte Carlo simulation. Accredit. Qual. Assur. 24, 417–426.

Karami, M.A., Fakhri, Y., Rezania, S., Alinejad, A.A., Mohammadi, A.A., Yousefi, M., Ghaderpoori, M., Saghi, M.H., Ahmadpour, M., 2019. Non-Carcinogenic health risk assessment due to fluoride exposure from tea consumption in Iran using Monte Carlo simulation. Int. J. Environ. Res. Public Health 16, 4261.

Khan, S., Munir, S., Sajjad, M., Li, G., 2016. Urban park soil contamination by potentially harmful elements and human health risk in Peshawar City, Khyber Pakhtunkhwa, Pakistan. J. Geochem. Explor. 165, 102–110.

Kurmus, H., Mohajerani, A., 2020. Leachate analysis of heavy metals in cigarette butts and bricks incorporated with cigarette butts. Materials 13, 2843.

Li, H., Yu, S., Li, G., Deng, H., Luo, X., 2011. Contamination and source differentiation of Pb in park soils along an urban–rural gradient in Shanghai. Environ. Pollut. 159, 3536–3544.

Li, X., Feng, L., 2012. Multivariate and geostatistical analyzes of metals in urban soil of Weinan industrial areas, Northwest of China. Atmos. Environ. 47, 58–65.

Li, X., Poon, C., Liu, P.S., 2001. Heavy metal contamination of urban soils and street dusts in Hong Kong. Appl. Geochem. 16, 1361–1368.

Li, Y., Yuan, Y., Sun, C., Sun, T., Liu, X., Li, J., et al., 2020. Heavy metals in soil of an urban industrial zone in a metropolis: risk assessment and source apportionment. Stoch. Environ. Res. Risk Assess. 34, 435–446.

Lin, Y., Ma, J., Zhang, Z., Zhu, Y., Hou, H., Zhao, L., et al., 2018. Linkage between human population and trace elements in soils of the Pearl River Delta: implications for source identification and risk assessment. Sci. Total Environ. 610–611, 944–950.

Liu, L., Liu, Q., Ma, J., Wu, H., Qu, Y., Gong, Y., et al., 2020. Heavy metal(loid)s in the topsoil of urban parks in Beijing, China: concentrations, potential sources, and risk assessment. Environ. Pollut. 260, 114083.

Liu, X., Zhong, L., Meng, J., Wang, F., Zhang, J., Zhi, Y., et al., 2018. A multi_medium chain modeling approach to estimate the cumulative effects of cadmium pollution on human health. Environ. Pollut. 239, 308–317.

Ma, W., Tai, L., Qiao, Z., Zhong, L., Wang, Z., Fu, K., et al., 2018. Contamination source apportionment and health risk assessment of heavy metals in soil around municipal solid waste incinerator: a case study in North China. Sci. Total Environ. 631, 348–357.

MEE, 2018. GB 36600-2018, Soil Quality Standard: Risk Control Standard for Soil Contamination of Development Land. Ministry of Ecology and Environment.

MEP, 2013. Soil and sediment - Determination of mercury, arsenic, selenium, bismuth, antimony - Microwave dissolution/Atomic Fluorescence Spectrometry. Ministry of Environmental Protection of China.

MohseniBandpi, A., Eslami, A., Ghaderpoori, M., Shahsavani, A., Jeihooni, A.K., Ghaderpoury, A., Alinejad, A., 2018. Health risk assessment of heavy metals on PM2.5 in Tehran air, Iran. Data Brief. 17, 347–355.

Muller, G., 1969. Index of geoaccumulation in sediments of the Rhine River. J. Geol. 2, 108–118.

Peng, T.Y., O'Connor, D., Zhao, B., Jin, Y.L., Zhang, Y.H., Tian, L., et al., 2019. Spatial distribution of lead contamination in soil and equipment dust at children's playgrounds in Beijing, China. Environ. Pollut. 245, 363–370.

Qu, C., Ma, Z., Yang, J., Liu, Y., Bi, J., Huang, L., 2012. Human exposure pathways of heavy metals in a lead-zinc mining area, Jiangsu Province, China. Plos One 7, 46793.

Rahman, M.S., Khan, M.D.H., Jolly, Y.N., Kabir, J., Akter, S., Salam, A., 2019. Assessing risk to human health for heavy metal contamination through street dust in the Southeast Asian Megacity: Dhaka, Bangladesh. Sci. Total Environ. 660, 1610–1622.

Ribeiro, A.P., Figueiredo, A.M.G., dos Santos, J.O., Dantas, E., Cotrim, M.E.B., Figueira, R.C.L., et al., 2013. Combined SEM/AVS and attenuation of concentration models for the assessment of bioavailability and mobility of metals in sediments of Sepetiba Bay (SE Brazil). Mar. Pollut. Bull. 68, 55–63.

Shepard, F., 1954. Nomenclature based on sand-silt-clay ratios. J. Sediment. Pet. 24, 151–158.

Shoari, N., Ezzati, M., Baumgartner, J., Malacarne, D., Fecht, D., 2020. Accessibility and allocation of public parks and gardens during COVID-19 social distancing in England and Wales. Plos One 15, 0241102.

SMSB, 2020. The 2019 shanghai national economic and social development statistical bulletin (in Chinese). Stat. Theory Pract. 3, 12–22.

Song, B., Guo, G.H., Lei, M., Wang, Y.W., 2018. Assessments of contamination and human health risks of heavy metals in the road dust from a mining county in Guangxi, China. Hum. Ecol. Risk Assess. 24, 1606–1622.

Tian, S.H., Liang, T., Li, K.X., Wang, L.Q., 2018. Source and path identification of metals pollution in a mining area by PMF and rare earth element patterns in road dust. Sci. Total Environ. 633, 958–966.

Tong, R., Yang, X., Su, H., Pan, Y., Zhang, Q., Wang, J., et al., 2018. Levels, sources and probabilistic health risks of polycyclic aromatic hydrocarbons in the agricultural soils from sites neighboring suburban industries in Shanghai. Sci. Total Environ. 616–617, 1365–1373.
TzuHsuen, Y., DengYuan, K., Joyce EnHua, W., ChangChuan, C., 2020. Associations between renal functions and exposure of arsenic and polycyclic aromatic hydrocarbon in adults living near a petrochemical complex. Environ. Pollut. 256, 113457.
USEPA, 1989. Risk Assessment Guidance for Superfund Volume I: Human Health Evaluation Manual (Part A). U.S. Environment Protection Agency (Washington DC).
USEPA, 2009. Risk Assessment Guidance for Superfund (RAGS). U.S. Environment Protection Agency (Washington DC).
USEPA, 2011. Exposure Factors Handbook, Final ed. U.S. Environment Protection Agency (Washington DC).
USEPA, 2014a. EPA Positive Matrix Factorization (PMF) 5.0 Fundamentals and User Guide. U.S. Environment Protection Agency (Washington DC).
USEPA, 2014b. Method 6020B (SW-846): Inductively Coupled Plasma-Mass Spectrometry. U.S. Environment Protection Agency (Washington DC).
Wallace, D.R., Taalab, Y.M., Heinze, S., Lovaković, B.T., Pizent, A., Renieri, E., et al., 2020. Toxic metal induced alteration in miRNA expression profile as a proposed mechanism for disease development. Cells 9, 2073–4409.
Wang, J.H., Li, S.W., Cui, X.Y., Li, H.M., Qian, X., Wang, C., et al., 2016. Bioaccessibility, sources and health risk assessment of trace metals in urban park dust in Nanjing, Southeast China. Ecotoxicol. Environ. Safe 128, 161–170.
Wang, M., Han, Q., Gui, C., Cao, J., Liu, Y., He, X., et al., 2019a. Differences in the risk assessment of soil heavy metals between newly built and original parks in Jiaozuo, Henan Province, China. Sci. Total Environ. 676, 1–10.
Wang, S., Cai, L.M., Wen, H.H., Luo, J., Wang, Q.S., Liu, X., 2019b. Spatial distribution and source apportionment of heavy metals in soil from a typical county-level city of Guangdong Province, China. Sci. Total Environ. 655, 92–101.
WHO, 2020. Lead Poisoning and Health. World Health Organization.
Xie, J., Luo, S., Furuya, K., Sun, D., 2020. Urban Parks as Green Buffers During the COVID-19 Pandemic. Sustainability 12, 6751.
Yadav, I.C., Devi, N.L., Singh, V.K., Li, J., Zhang, G., 2019. Spatial distribution, source analysis, and health risk assessment of heavy metals contamination in house dust and surface soil from four major cities of Nepal. Chemosphere 218, 1100–1113.
Yang, S., Zhao, J., Chang, S.X., Collins, C., Xu, J., Liu, X., 2019. Status assessment and probabilistic health risk modeling of metals accumulation in agriculture soils across China: a synthesis. Environ. Int. 128, 165–174.
Yao, B., Lu, X., Xu, L., Wang, Y., Qu, H., Zhou, H., 2020. Relationship between low-level lead, cadmium and mercury exposures and blood pressure in children and adolescents aged 8–17 years: an exposure-response analysis of NHANES 2007–2016. Sci. Total Environ. 726, 0048–9697.
Zarezadeh, R., Rezaee, P., Lak, R., Masoodi, M., Ghorbani, M., 2017. Distribution and accumulation of heavy metals in sediments of the northern part of mangrove in Hara biosphere reserve, Qeshm Island (Persian Gulf). Soil Water Res 12, 86–95.
Zhang, C., 2005. Using multivariate analyses and GIS to identify pollutants and their spatial patterns in urban soils in Galway, Ireland. Environ. Pollut. 142, 501–511.
Zhang, R., Chen, T., Zhang, Y., Hou, Y., Chang, Q., 2020. Health risk assessment of heavy metals in agricultural soils and identification of main influencing factors in a typical industrial park in northwest China. Chemosphere 252, 126591.
Zhang, X., Wei, S., Sun, Q., Wadood, S.A., Guo, B., 2018. Source identification and spatial distribution of arsenic and heavy metals in agricultural soil around Hunan industrial estate by positive matrix factorization model, principle components analysis and geo statistical analysis. Ecotoxicol. Environ. Safe 159, 354–362.
Zhou, Y.T., Niu, L.L., Liu, K., Yin, S.S., Liu, W.P., 2018. Arsenic in agricultural soils across China: distribution pattern, accumulation trend, influencing factors, and risk assessment. Sci. Total Environ. 616, 156–163.
Zhuang, W., Wang, Q., Tang, L., Liu, J., Yue, W., Liu, Y., et al., 2018. A new ecological risk assessment index for metal elements in sediments based on receptor model, speciation, and toxicity coefficient by taking the Nansihu Lake as an example. Ecol. Indic. 89, 725–737.